

AD A 025291

FG  
12

DEVELOPMENT OF AN OPTICAL DISC RECORDER

QUARTERLY TECHNICAL REPORT

1 January 1976 to 31 March 1976

Sponsored by

ADVANCED RESEARCH PROJECTS AGENCY

ARPA Order No. 3080  
Program Code No. 6D30

Contract No. N00014-76-C-0441

Principal Investigator: George Kenney (914) 762-0300

Scientific Officer: Marvin Denicoff

Amount of Contract: \$700 719

Contract Period: 1 Oct. 1975 - 31 March 1977

THE VIEWS AND CONCLUSIONS CONTAINED IN THIS DOCUMENT  
ARE THOSE OF THE AUTHORS AND SHOULD NOT BE INTERPRETED  
AS NECESSARILY REPRESENTING THE OFFICIAL POLICIES,  
EITHER EXPRESSED OR IMPLIED, OF THE ADVANCED RESEARCH  
PROJECTS AGENCY OR THE U.S. GOVERNMENT.

DDC  
RECEIVED  
JUN 9 1976  
RECEIVED

Prepared by

PHILIPS LABORATORIES

A Division of North American Philips Corporation  
Briarcliff Manor, New York 10510

g

A

6 May 1976

DISTRIBUTION STATEMENT A  
Approved for public release;  
Distribution Unlimited

UNCLASSIFIED

SECURITY CLASSIFICATION OF THIS PAGE (When Data Entered)

REPORT DOCUMENTATION PAGE		READ INSTRUCTIONS BEFORE COMPLETING FORM
1. REPORT NUMBER	2. GOVT ACCESSION NO.	3. RECIPIENT'S CATALOG NUMBER
4. TITLE (and Subtitle)		5. TYPE OF REPORT & PERIOD COVERED
DEVELOPMENT OF AN OPTICAL DISC RECORDER.		Quarterly Technical Report, 1 Jan 1976 - 31 Mar 1976
6. AUTHOR(s)		7. PERFORMING ORG. REPORT NUMBER
G. Kenney, C. Balas, D. Lou, A. Chan, T. Demetrakopoulos, R. McFarlane, J. Wagner, P. Janssen		PL-21-VR76-0507
9. PERFORMING ORGANIZATION NAME AND ADDRESS		8. CONTRACT OR GRANT NUMBER(s)
Philips Laboratories A Division of North American Philips Corp. Briarcliff Manor, New York 10510		N00014-76-C-0441
11. CONTROLLING OFFICE NAME AND ADDRESS		10. PROGRAM ELEMENT, PROJECT, TASK AREA & WORK UNIT NUMBERS
Advanced Research Projects Agency 1400 Wilson Blvd. Arlington, Virginia 22209		ARPA Order No. 3080 Program Code No. 6D30
14. MONITORING AGENCY NAME & ADDRESS (if different from Controlling Office)		12. REPORT DATE
Office of Naval Research 800 North Quincy Street Arlington, Virginia 22217 Code: 437		11 May 1976
16. DISTRIBUTION STATEMENT (of this Report)		13. NUMBER OF PAGES
		40
17. DISTRIBUTION STATEMENT (of this abstract entered in Block 20, if different from Report)		15. SECURITY CLASS. (of this report)
		UNCLASSIFIED
18. SUPPLEMENTARY NOTES		15a. DECLASSIFICATION/DOWNGRADING SCHEDULE
19. KEY WORDS (Continue on reverse side if necessary and identify by block number)		
optical disc recorder direct read after write (DRAW) lasers substrate materials		recording materials disc protective mechanism disc for an optical disc recorder.
20. ABSTRACT (Continue on reverse side if necessary and identify by block number)		
A program schedule with milestones is given for the materials development and recorder construction. This schedule will be used, updated where necessary, on all subsequent reports. The recorder components were fabricated, and the recorder is being assembled. Laser machining of bismuth and selenium films produced at PL indicates acceptable sensitivity and hole geometries. The air sandwich appears to be the most attractive protective mechanism for the disc and has been chosen as the prime candidate for extensive testing and analysis. A task force was set up to study digital coding problems.		

DD FORM 1473

EDITION OF 1 NOV 65 IS OBSOLETE

UNCLASSIFIED

SECURITY CLASSIFICATION OF THIS PAGE (When Data Entered)

387 334 ✓



QUARTERLY TECHNICAL REPORT  
1 January 1976 to 31 March 1976

1. SUMMARY

A program schedule with milestones is given for the materials development and recorder construction. This schedule will be used, updated where necessary, on all subsequent reports. The recorder components were fabricated, and the recorder is being assembled. Laser machining of bismuth and selenium films produced at PL indicates acceptable sensitivity and hole geometries. The air sandwich appears to be the most attractive protective mechanism for the disc and has been chosen as the prime candidate for extensive testing and analysis. A task force was set up to study digital coding problems.

2. RESEARCH PROGRAM OBJECTIVES

The objective of this program is to develop an optical disc recorder of digital information, with a direct-read-after-write (DRAW) capability. A storage capacity of  $> 10^{10}$  bits is desired, with  $4.4 \times 10^5$  bits on each of the 40,000 tracks of the disc. The desired error rate is  $10^{-9}$  at a data rate greater than 1 M bit/sec. The key element in the proposed system is a recording material that can be exposed with a low-cost, low-power laser (e.g., HeNe) - leading to a recorder which could be manufactured for  $< \$10,000$  and discs which would cost  $< \$10$  in quantity.

3. SCHEDULE

The program schedule and milestones given in Figure 1 are for both materials development and recorder construction. On or by May 15, the first narrowing of material choices based on static hole-burning measurements will be made. A second decision point will depend on the results of dynamic testing of the



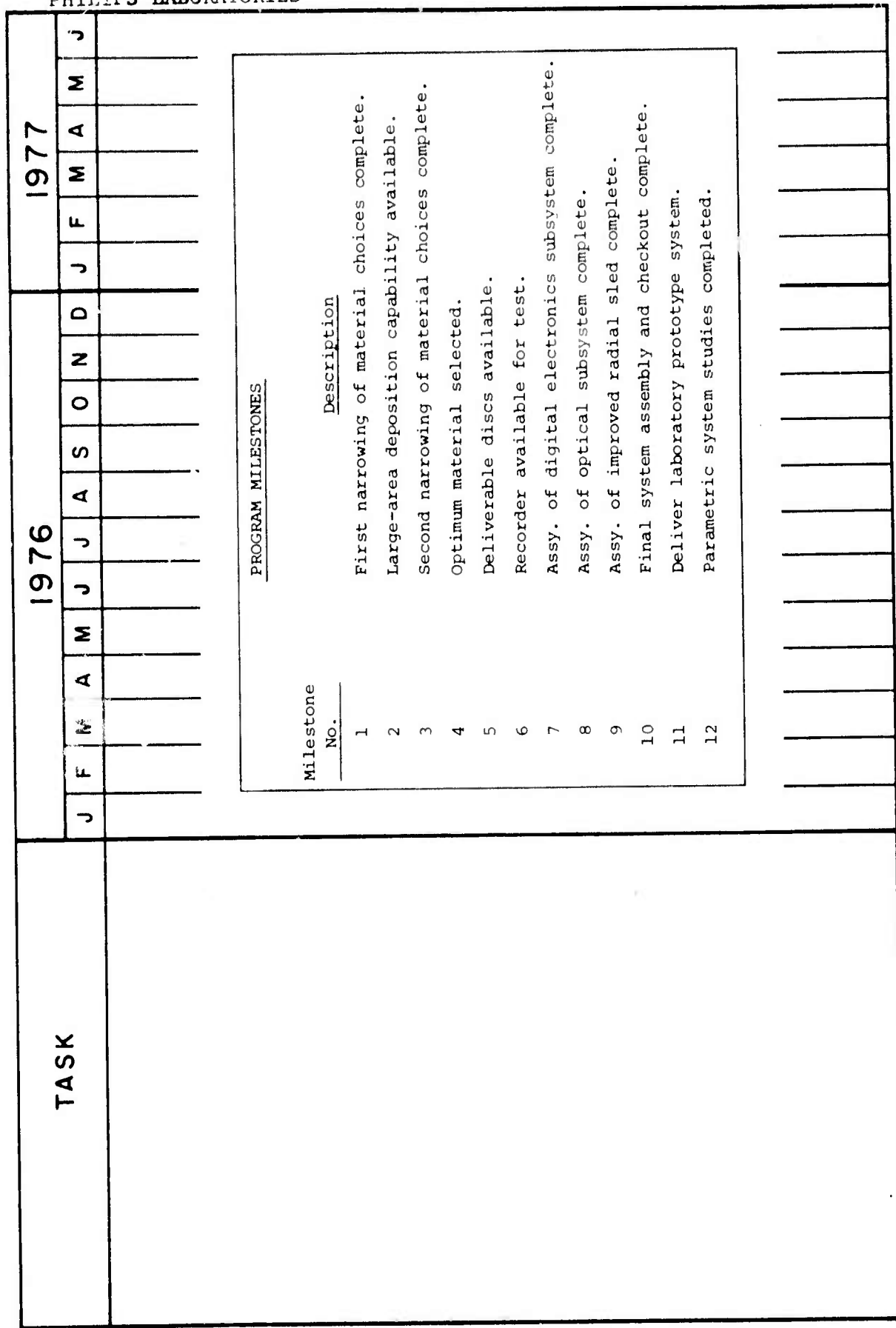


Figure 1: Program Schedule for Development of Optical Disc Recorder (sht. 2 of 2)

## PHILIPS LABORATORIES

materials deposited on discs. The dynamic testing includes measurements of signal-to-noise ratios and defects; this testing requires an operational recorder as a test vehicle. The results of the dynamic testing and the materials development phase should allow a final material selection by January 1, 1977. During the material development phase, uniform deposition techniques for large areas will be investigated, and special consideration will be given to any interaction between those techniques and the protective mechanism (i.e., air sandwich) for the disc.

A parallel effort to design and construct a laboratory-model recorder is also outlined in the schedule (Fig. 1). The recorder is a key requirement for adequate testing of DRAW materials and for evaluation of the disc protective mechanism. Construction of the recorder is also necessary to evaluate new mechanical techniques, such as the air bearing sled and turntable, which are needed for the design of an engineering model to meet the program goals.

The first tests will be the recording of analog TV signals with a 200 mW argon laser, at a disc speed of 30 rps. These conditions were chosen because they represent our experience so far with VLP<sup>®\*</sup> video disc recorders developed by the Philips Research Laboratory in Eindhoven, Netherlands. This test is in some respects more demanding than that of recording digital signals; for example, the signal-to-noise ratio required for acceptable video recording is much higher than that for the proposed digital recording. Once the recorder has performed satisfactorily by recording a video disc, the recorder will be refitted for digital recording with a low-power HeNe laser and for operation at slower disc speeds. The refitting program requires the design of digital record/playback electronics, an improved slow motion sled, and a low-power, red, optical subsystem. The digital record/playback electronics must include proper channel equalization, error detection, and error correction. It is first necessary to characterize the channel

---

\*registered trademark of N.V. Philips, Holland.

## PHILIPS LABORATORIES

and then choose the proper coding scheme.

A task force to study digital coding has been set up in cooperation with Philips Research Laboratory in the Netherlands, and with the Magnavox Company. They will study the following problems:

- Bit error detection and measuring techniques.
- Choice of coding modulation.
- Choice of registration code.
- Corrective techniques affecting coding modulation and registration code.
- Read-out techniques and channel equalization.
- Timebase stability and bit slip.
- Other channel characteristics such as signal-to-noise ratio, track-to-track crosstalk, and intersymbol interference.
- Hardware considerations.

4. PROGRESS AND DISCUSSION

Assembly of the recorder was completed (see Fig. 2). The assembled sled, turntable, and velocity transducer are being tested. The initial tests will be with a 200 mW argon laser at a disc speed of 30 rps.

Tests of the sled speed are being conducted. With the optics tray installed, holes are being machined on a stationary microscope slide covered with a layer of bismuth. Figure 3 shows holes machined with a sled speed of 45  $\mu\text{m}/\text{sec}$ . Judging from the uniformity of the hole spacing, it can be said that at this speed the sled speed control is adequate.

The motor speed-control servo electronics were system tested and performed satisfactorily. The stability of the turntable speed was found to be 0.01% per  $^{\circ}\text{C}$ ; the tachometer error is less than 1 part in 10,000. The focusing and radial-tracking servo electronics were fabricated and bench tested. Systems testing will begin in May.

Members of the digital-coding task force will meet at FL on May 19-20, 1976. At that time, the results of an initial channel characterization will be presented and a more definitive program established.

The air sandwich appears to be the most attractive mechanism for protecting the disc and has been chosen as the prime candidate for extensive testing and analysis. An air sandwich was constructed using two VLP discs to determine whether the lamination affected the playback quality. Critical electrical performance data were taken before and after lamination. The details of these tests are presented in Appendix I. It was found that the picture quality did not change appreciably from the original single-sided discs. The test is in some respects more demanding than that for digital signals; for example, the S/N ratio required for acceptable video recording is much higher than that required for the proposed digital recording.

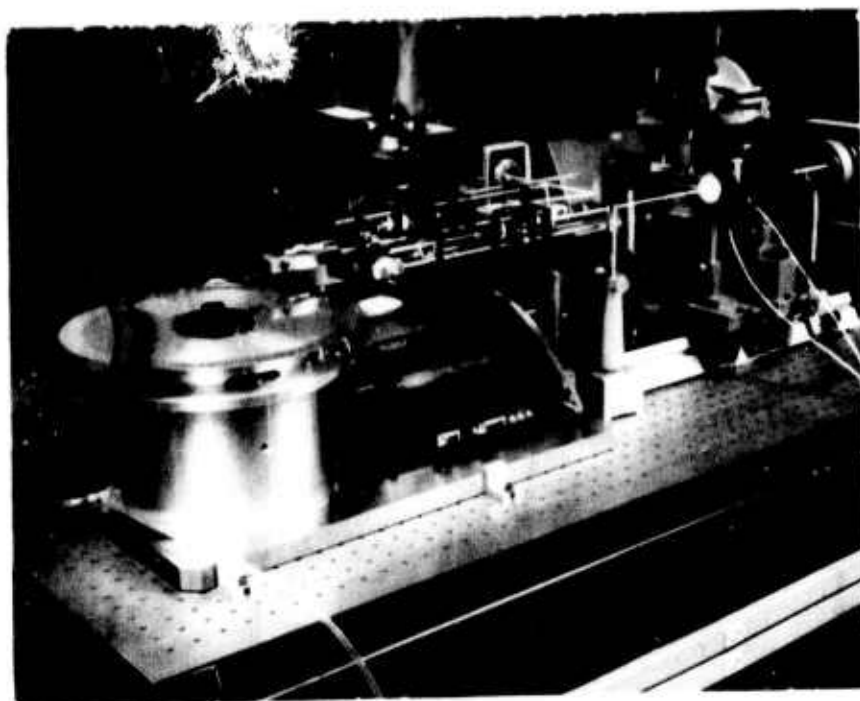


Figure 2: Assembled Recorder.

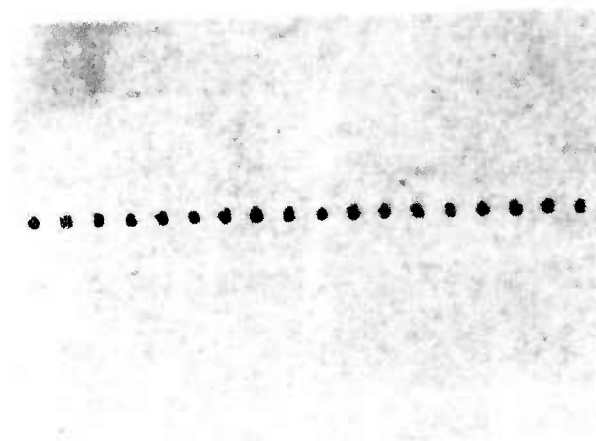


Figure 3:  $1\ \mu\text{m}$  holes machined in bismuth ( $V = 45\ \mu\text{m}/\text{sec}$ ).

## PHILIPS LABORATORIES

The effects of time, temperature, operating speed, etc., must still be considered.

Analytical and experimental work to evaluate the air sandwich lamination is in progress to determine optimum material and structural configurations. One initial result of the analytical study (see Appendices II and III) is a capability for predicting deflections of the air sandwich as a function of speed, disc radius, thickness, sealing, etc. The predicted deflections for a sealed air sandwich are only a few microns and should present no problems for the focusing servo system.

Preliminary evaluation of the sensitivity and hole profiles of candidate materials bismuth and selenium was completed. The evaluation was carried out at 488 nm with a 0.8  $\mu\text{m}$  diameter laser beam at 750  $\mu\text{s}$  pulse exposure. The surface power required to form 0.8  $\mu\text{m}$  holes is 7 mW for bismuth and 2 mW for selenium (Note, this testing was done with blue 488 nm light; for machining with red 633 nm light, the hole size would be about 1  $\mu\text{m}$ ). Both bismuth and selenium are, therefore, acceptable as recording media for the proposed application. Bismuth will require a system optical transmission of 70% with a 20 mW He-Ne laser, while selenium will require the use of a He-Cd laser. One low-melting point material, tellurium, is also being studied at PL. Difficulties in depositing good films of cadmium and antimony have, in effect, forced us to narrow the material field at this time. Philips Research Laboratories in the Netherlands will look at other promising red-sensitive DRAW materials.

5. PLANS FOR NEXT QUARTER

- a. Test recorder by recording analog TV signals with a 200 mW argon laser, at a disc speed of 30 rps.
- b. Continue program to refit recorder for digital operation with a low-power laser and for slower disc speeds.
- c. Continue characterization of low boiling point materials, bismuth and tellurium.
- d. Make first selection of DRAW material based on sensitivity and hole profiles (5/15/76).
- e. Study digital coding problems.
- f. Propose a program, subject to ARPA approval, for archival testing of bismuth and tellurium films.

APPENDIX I

PRELIMINARY FINDINGS ON AIR SANDWICH LAMINATED VLP DISCS

APPENDIX I  
PRELIMINARY FINDINGS ON AIR SANDWICH LAMINATED VLP DISCS

by

A. Y. Chan  
C. Balas  
P. Tasaico  
L. Skala  
L. Irizarry

Two VLP discs were laminated with an air space between them to determine whether this double-sided configuration could be played and still maintain high quality. The critical electrical performance data taken before and after laminating are described. The discs were played on our "BERLIN" VLP player No. 6.

1. Electrical Performance

A PAL disc and an NTSC (direct system) disc were selected for the experiment. Before laminating the selected VLP discs, pictures were obtained of the monitor video display, the FM envelope from the output of the preamplifier, and the focusing servo error signal. On the PAL disc, the above data, collected at a radius of 12.4 cm, is shown in Fig. 1-A. Similar data was collected from an NTSC disc at radii of 12.4 cm and 7.3 cm, as shown in Figs. 2-A and 3-A, respectively. In addition, each disc was individually played in the normal mode to obtain an overall impression of the quality of the monitor video display.

After laminating the two discs, an evaluation followed. In the normal playback mode, the video display quality, including time-base stability of each side, was found to be very close to that before laminating. The playback data after laminating is shown in Figs. 1-B, 2-B and 3-B.

The focusing servo error was observed to have higher frequency components. Minor adjustment was made in the focusing servo gain control. No adjustment on the motor control servo nor the radial servo was necessary.

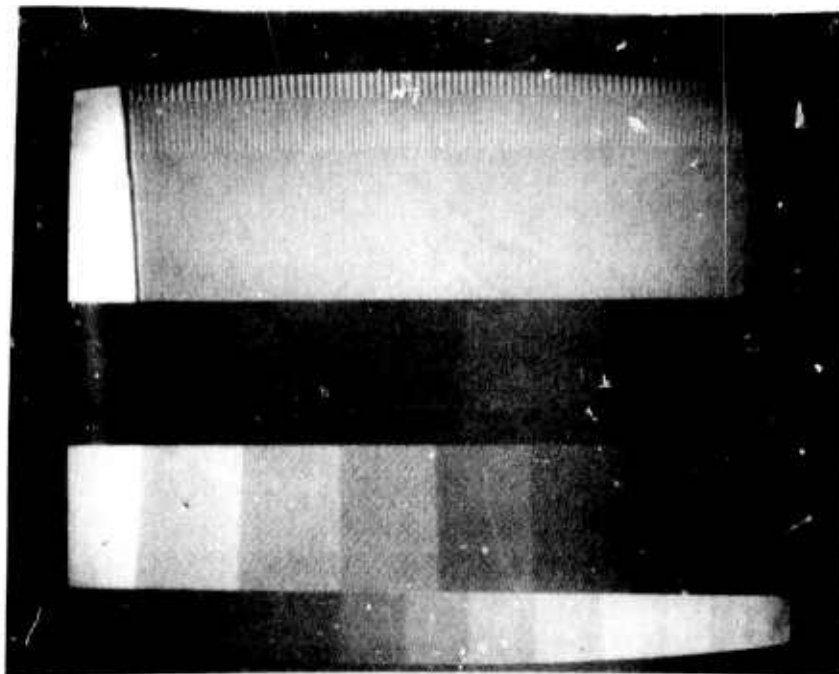
2. Mechanical

The particular "air sandwich" lamination that was evaluated is shown in Figure 4. It consists of two VLP discs separated by an air space; standoffs placed between the discs at their inner and outer diameters create the air space. The standoffs and, therefore, the air space are 381  $\mu\text{m}$  thick.

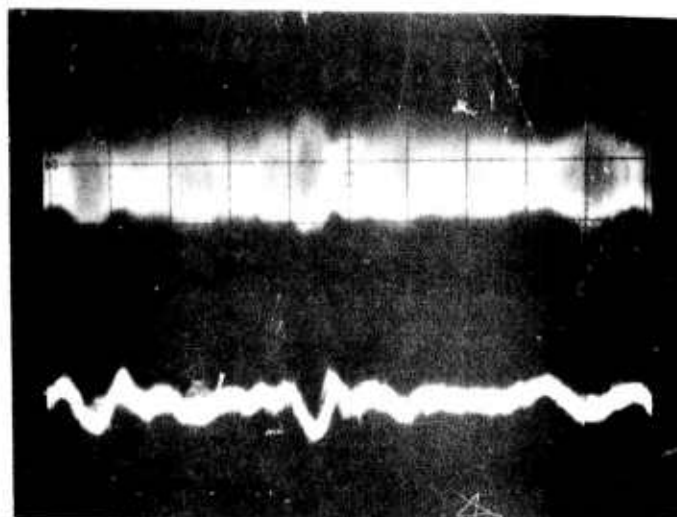
3. Conclusions

It was found that a double-sided disc could be made by laminating two VLP discs together in an air sandwich, and that the picture quality did not change appreciably from the original single-sided discs. The effects of time, temperature, operating speed, etc. must still be considered. Analytical and experimental work to evaluate the air sandwich lamination is in progress to determine optimum material and structural configurations.

Fig. 1-A. PAL DISC  
(before sandwiching)  
Radius = 12.4 cm



Monitor Display

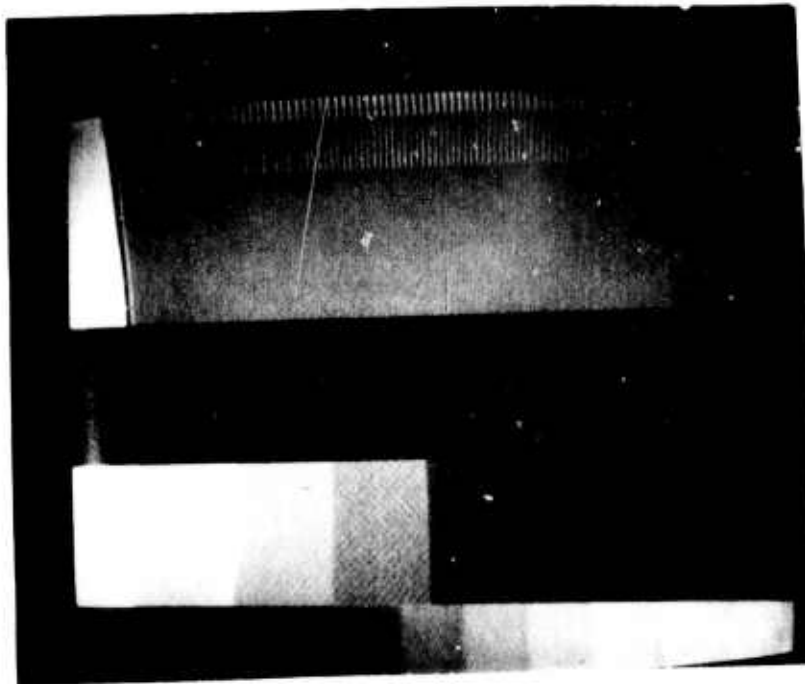


A. FM Envelope at  
Preamplifier Output

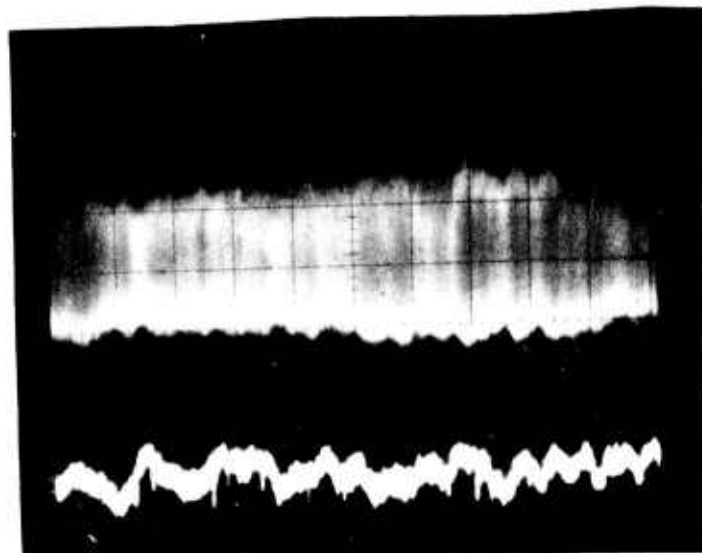
B. Focusing servo error  
signal

Vertical 50 mV/div.  
Horizontal 2 msec/div.

Fig. 1-B. PAL DISC  
(after sandwiching)  
R = 12.4 cm



Monitor Display



A. FM Envelope at  
Preamplifier Output

B. Focusing servo error  
signal

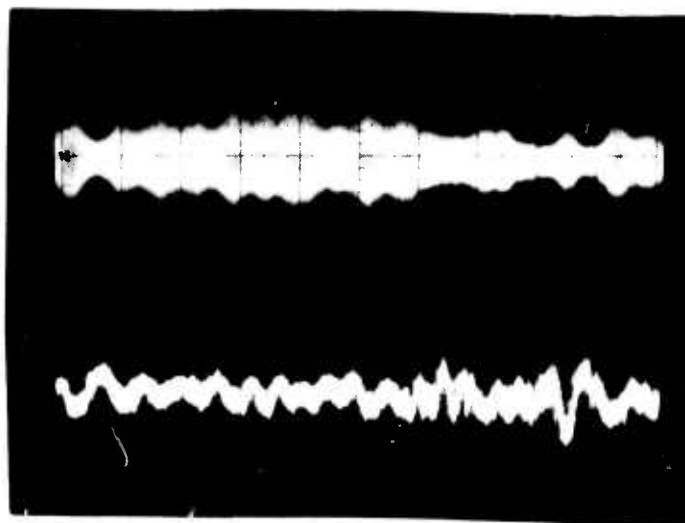
Vertical 50 mV/div.  
Horizontal 2 msec/div.

Fig. 2-A. NTSC DISC  
(before sandwiching)

R = 12.4 cm



Monitor Display



A. FM Envelope at  
Preamplifier Output

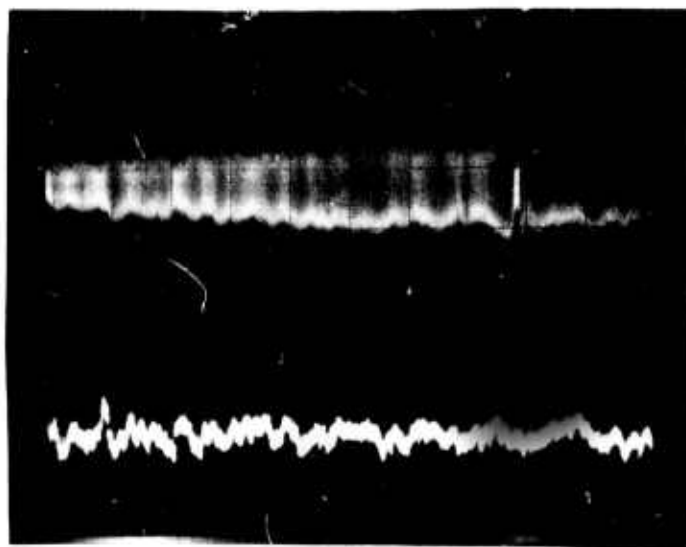
B. Focusing servo error  
signal

Vertical 50 mV/div.  
Horizontal 2 msec/div.

Fig. 2-B. NTSC DISC  
(after sandwiching)  
R = 12.4 cm



Monitor display



A. FM Envelope at  
Preamplifier Output

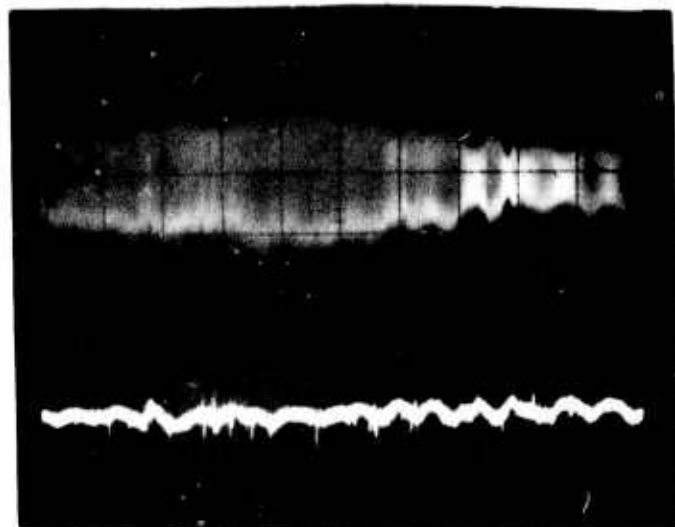
B. Focusing servo error  
signal

Vertical 50 mV/div.  
Horizontal 2 msec/div.

Fig. 3-A. NTSC DISC  
(before sandwiching)  
R = 7.3 cm



Monitor display



A. FM Envelope at  
Preamplifier Output

B. Focusing servo error  
signal

Vertical 50 mV/div.  
Horizontal 2 msec/div.

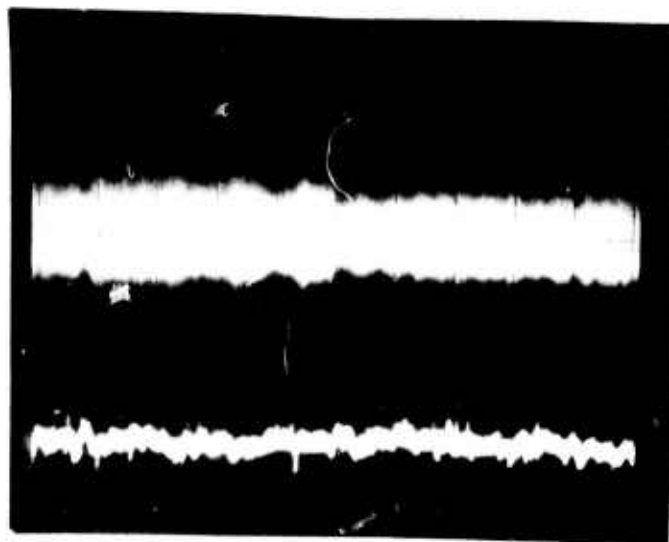
Fig. 3-B. NTSC DISC

(after sandwiching)

R = 7.3 cm



Monitor display



A. FM Envelope at  
Preamplifier Output

B. Focusing servo error  
signal

Vertical 50 mV/div.  
Horizontal 2 msec/div.

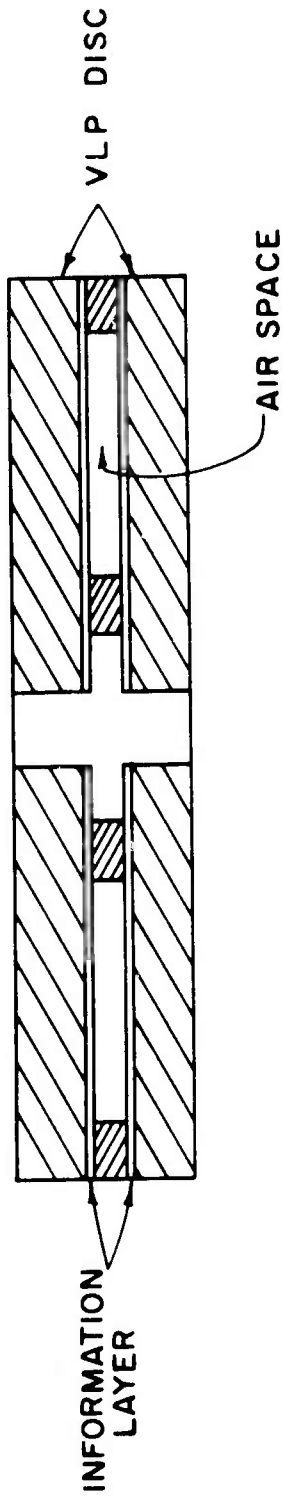


Fig. 4. The air-sandwich lamination.

APPENDIX II

STATUS OF ANALYSIS OF AIR-SANDWICH DISC

STATUS OF ANALYSIS OF AIR-SANDWICH DISK

by

John Wagner

1. CAVITY PRESSURE

The pressure distribution within the cavity of an air-sandwich type of disk was determined for various boundary conditions. Typical pressure profiles are illustrated in Figure 1, where  $P_{ss}$  represents the steady state pressure and  $P_{atm}$  refers to atmospheric pressure. The detailed analysis is given in Appendix III.

2. STRUCTURAL BEHAVIOR

2.1 Transverse Deflection Analysis

An elastic analysis of the transverse deformation due to a uniform cavity pressure was done. Numerical results for various cases were computed. For those cases where comparison is valid, the results agree with available classical solutions. The predicted transverse displacements ( $W$ ) for one of the cases are shown in Figure 2. Although the actual cavity pressure distribution is not uniform, the pressure level in Figure 2 was adjusted to give about the same maximum deflections as would be encountered in the actual case. In practice, the maximum displacement will occur more nearly in the center of the annular band than the profile due to uniform pressure (Fig. 2). Several additional considerations were then incorporated in the analysis.

Cavity pressure has been assumed to vary linearly with radius. In addition, the influence of deflection on the cavity volume and therefore pressure has now been included in the analysis. The combined effect of these two modifications on the deflections has been significant. Figure 3 illustrates typical results for a single cavity disk which was sealed at

atmospheric pressure and is spinning at 1800 rpm. Figure 4 illustrates the transverse deflections that occur for a similar disk the cavity of which is vented to the atmosphere at the inner radius. The ability of the cavity to exchange air with the atmosphere as its volume changes results in a pressure distribution which does not vary with deflection. As a result, the deflections are considerably larger than those shown in Figure 3. Alternatively, if the cavity is vented to the atmosphere at the outer radius, the glass and plastic will be sucked together. In order to determine the stress field associated with the deflections, a subroutine is currently being added to the computer program.

## 2.2 Radial Deflection Analysis

An elastic analysis of the radial deformations and associated in plane stresses for various DRAW disk configurations was completed during the reporting period. Typical results are shown in a disk segment in Figure 5. The disk in Figure 5 is of the same configuration, dimensions, and materials as the disk in the previous figures. In this particular case the hub is simply an epoxy bonded laminate of the glass and plastic sheets. However, the computer program is general and allows for a variety of materials. The analysis is now being extended to include hub clamping forces and tapered spindle holes.

## 2.3 Spin Testing

A test has been devised to indirectly measure the creep compliance of individual plastic disks. It consists of spinning a plastic disk at constant speed and measuring the radial displacement. Measurements along two different diameters will be made at prescribed time intervals. By this procedure playing cycles can be simulated and therefore both creep and recovery behavior studied. The experimental apparatus is being assembled and test disks are being cut from Westlake Polycarbonate and Glasflex PMMA.

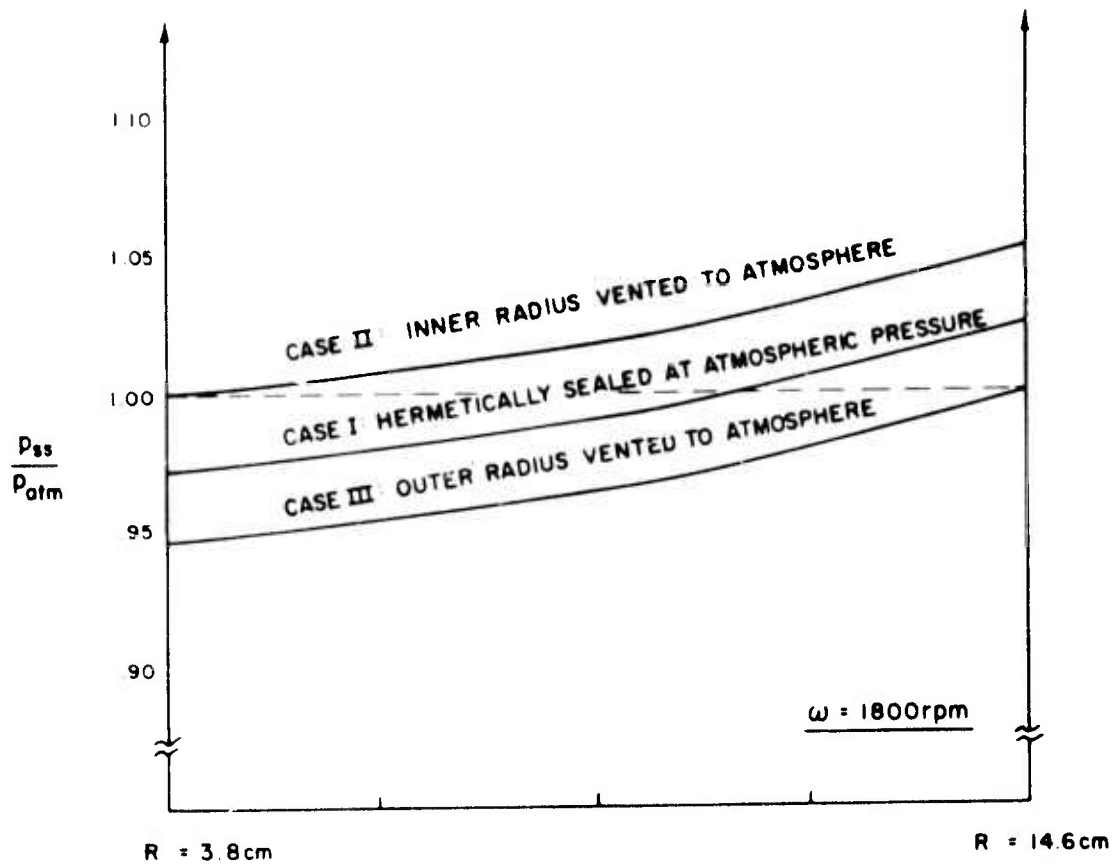


Figure 1: Cavity Pressure Profiles - Rigid Cavity

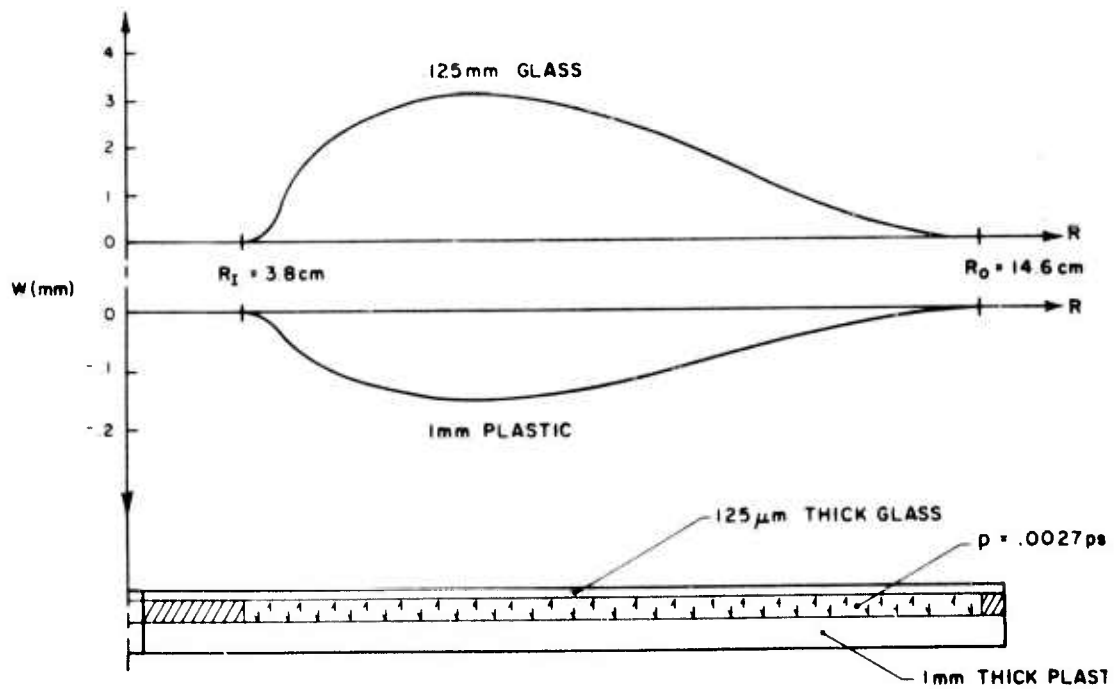


Figure 2: Transverse Deflections - Uniform Cavity Pressure

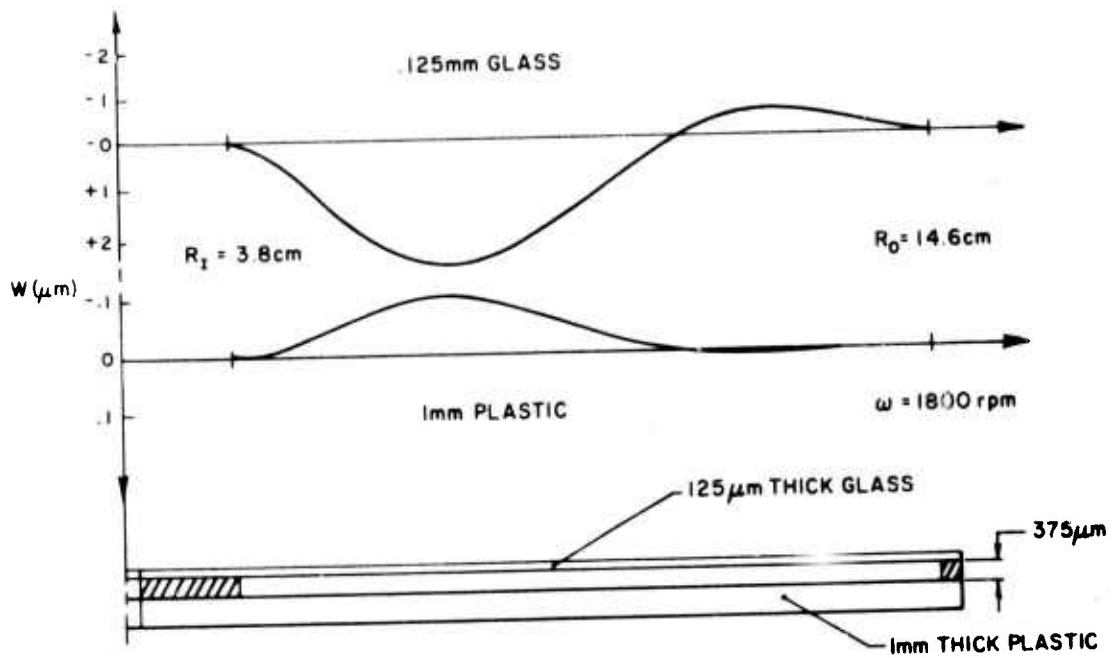


Figure 3: Transverse Deflections - Spinning Hermetic Cavity

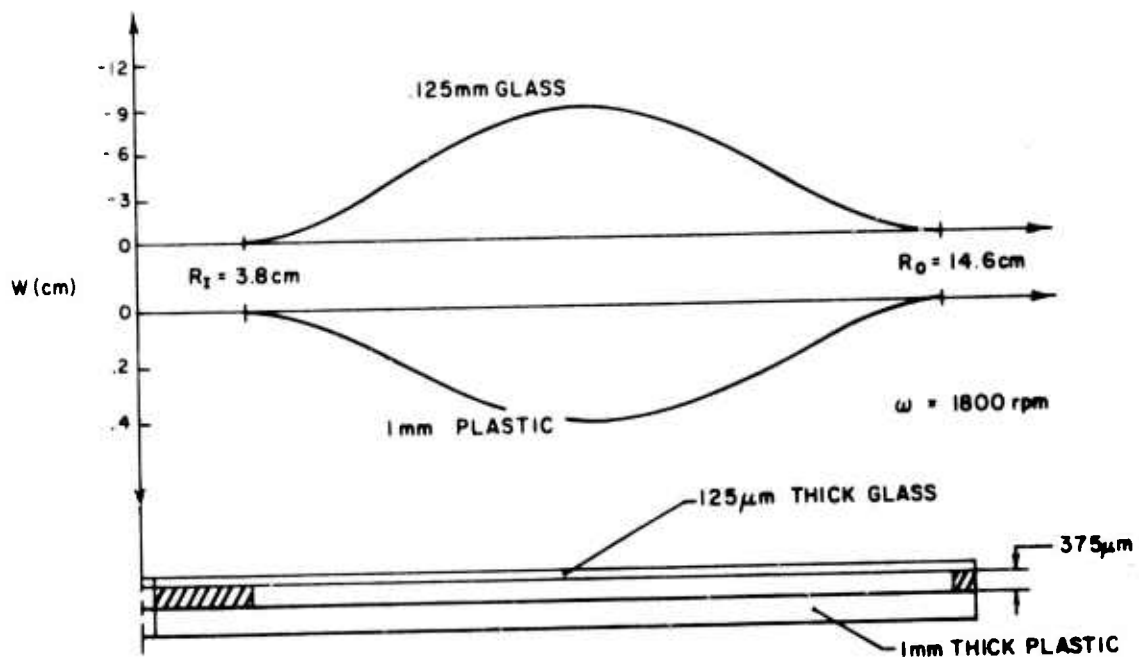


Figure 4: Transverse Deflections - Spinning Cavity Vented at  $R = R_I$

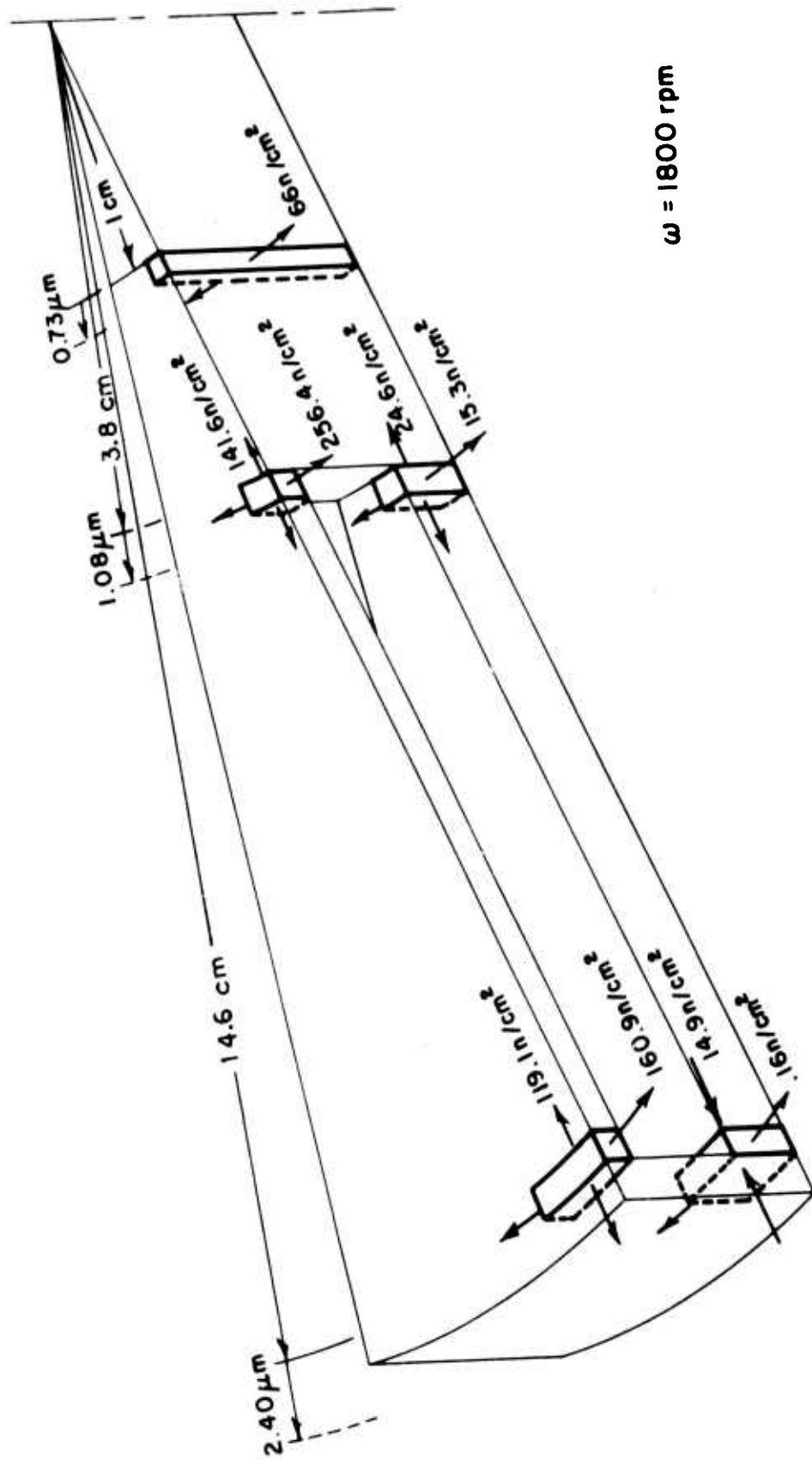


Figure 5: Stresses and Radial Deformations - Spinning Draw Disk

APPENDIX III

PRESSURE DISTRIBUTION IN THE CAVITY OF A DRAW AIR SANDWICH DISC

PHILIPS LABORATORIES

PRESSURE DISTRIBUTION IN THE CAVITY OF A DRAW AIR SANDWICH DISK

by John Wagner

INTRODUCTION

Spinning a DRAW Air Sandwich Disk causes within the cavity a pressure distribution which is different from the static distribution. This effect is due to the centrifugal force acting on the rotating air mass. C. Balas\* has analyzed approximately the pressure distribution under steady state conditions. The following study is a refinement and extension of his analysis. The principal refinement has been treating the air mass as compressible. In addition, the results are applicable to a variety of possible boundary conditions.

ASSUMPTIONS

The following conditions are assumed to be representative of the actual situation: 1) the gas within the cavity obeys the Ideal Gas Law; 2) in the steady state, the entire volume of gas within the cavity rotates as a rigid body with the same angular speed as that of the disk; 3) gravitational forces are negligible; and 4) the cavity is not deformable.

SUMMARY OF RESULTS

Under the assumed conditions, the steady state pressure ( $p_{SS}$ ) varies with radius (R) and disk speed ( $\omega$ ) in the following manner:

$$p_{SS} = Ae^{B\omega^2 R^2}$$

\* C. Balas, Internal Memorandum to G. Kenney, Philips Laboratories, June 2, 1975.

## PHILIPS LABORATORIES

For a typical VLP application, the steady state pressure increases about 6% in going from the inner radius to the outer radius of the cavity. The analysis is applicable to an initially pressurized (or evacuated) hermetic cavity as well as a cavity vented to the atmosphere.

### ANALYSIS

Along any one streamline, Euler's Equation requires that:

$$d\left(C_1 \frac{v^2}{2}\right) + \frac{1}{\rho} dp = 0 \quad (1)$$

where:  $p$  = absolute pressure  
 $\rho$  = mass density of gas  
 $v$  = speed along streamline  
 $C_1$  = conversion factor

In addition, the Ideal Gas Law requires that:

$$\frac{1}{\rho} = \frac{RT}{pM} \quad (2)$$

where:  $R$  = Universal Gas Constant  
 $M$  = molecular weight  
 $T$  = gas temperature

Therefore, if equations (1) and (2) are combined by the elimination of the density and by integration, the expression:

$$C_1 \frac{v^2}{2} + \frac{M}{RT} \ln p \quad (3)$$

must be constant along any one streamline. The variation of the constant from one streamline to another is given by Bernoulli's equation:

$$C_1 \rho \omega^2 r = \frac{\partial p}{\partial r} \quad (4)$$

where:  $r$  = radius of curvature of streamline.

Combining equations (2) and (4) with condition (3) results in a single governing differential equation:

$$\frac{dp}{p} = \frac{C_1 M}{RT} \omega^2 r dr \quad (5)$$

The detailed development of equation (5) is given in Appendix A.

Three specific cases are of potential importance in the DRAW disk application of equation (5).

#### Case I - Hermetic Cavity

Imagine the annual cavity (Figure 1) to be initially pressurized, or evacuated, to an absolute pressure level  $p_0$ . If equation (5) is integrated from the inner radius of the cavity to some arbitrary radius  $R$ ; the steady state pressure at  $R$  is expressed in terms of the steady state pressure at the inner radius of the cavity as:

$$p_{ss} = p_I e^{\frac{C_1 M \omega^2}{2RT} (R^2 - R_I^2)} \quad (6)$$

PHILIPS LABORATORIES

In order that the pressure  $p_I$  may be evaluated in terms of the static pressure  $p_O$ , the conservation of mass principle is applied to the confined gas:

$$\rho_O V_C = \text{mass of confined gas} = \int_{R_I}^{R_O} \rho_{SS} (2\pi r \delta) dr \quad (7)$$

where:  $V_C$  = cavity volume =  $\pi(R_O^2 - R_I^2)\delta$   
 $\rho_{SS}$  = steady state gas density  
 $\rho_O$  = static gas density  
 $\delta$  = cavity thickness

If equations (2), (6), and (7) are combined and integrated over the limits from  $R_I$  to  $R_O$ , then:

$$p_{SS} = \frac{C_1 M \omega^2 (R_O^2 - R_I^2) e^{\frac{C_1 M \omega^2 (R^2 - R_I^2)}{2RT}}}{2RT \left[ e^{\frac{C_1 M \omega^2 (R_O^2 - R_I^2)}{2RT}} - 1 \right]} p_O \quad (8)$$

For a detailed development of equation (8) refer to Appendix B.

A numerical example of the pressure distribution described by equation (8) is illustrated in Figure 2. The data used are given below:

$R_I$  = 1.5 in = 3.81 cm  
 $R_O$  = 5.75 in = 14.61 cm  
 $T$  = 23°C  
 $C_1$  =  $0.987 \times 10^{-6}$  atm cm<sup>2</sup>/dyne  
 $\underline{R}$  = 82.07 (cm<sup>3</sup> atm)/(mole °C)  
 $M$  = 29 grams/mole of air

$p_{ss}/p_o$ , eqn. (8)		R (cm)
$\omega = 1800$ rpm	$\omega = 3600$ rpm	--
.9728	.8967	3.81
.9801	.9246	6.51
.9914	.9688	9.21
1.0067	1.0315	11.91
1.0263	1.1161	14.61

Case II - Cavity Vented to the Atmosphere at  $R = R_I$

If equation (5) is integrated from the inner radius of the cavity to some arbitrary radius R; the steady state pressure at R can be expressed in terms of the steady state pressure at the inner radius of the cavity. In this case, the pressure at  $R = R_I$  is atmospheric pressure ( $p_{atm}$ ):

$$p_{ss} = p_{atm} e^{\frac{C_1 M_w^2 (R^2 - R_I^2)}{2RT}} \quad (9)$$

Case III - Cavity Vented to the Atmosphere at  $R = R_O$

The reasoning of Case II applies to Case III. The resulting expression is:

$$p_{ss} = p_{atm} e^{\frac{C_1 M_w^2 (R^2 - R_O^2)}{2RT}} \quad (10)$$

## PHILIPS LABORATORIES

In both Cases II and III, the pressure distribution is the same as that for a hermetic cavity. However, in Case II the pressure is everywhere above (or equal to) atmospheric whereas in Case III the pressure is everywhere below (or equal to) atmospheric.

### ACKNOWLEDGEMENT

I would like to thank Stephen Ross for his helpful discussions.

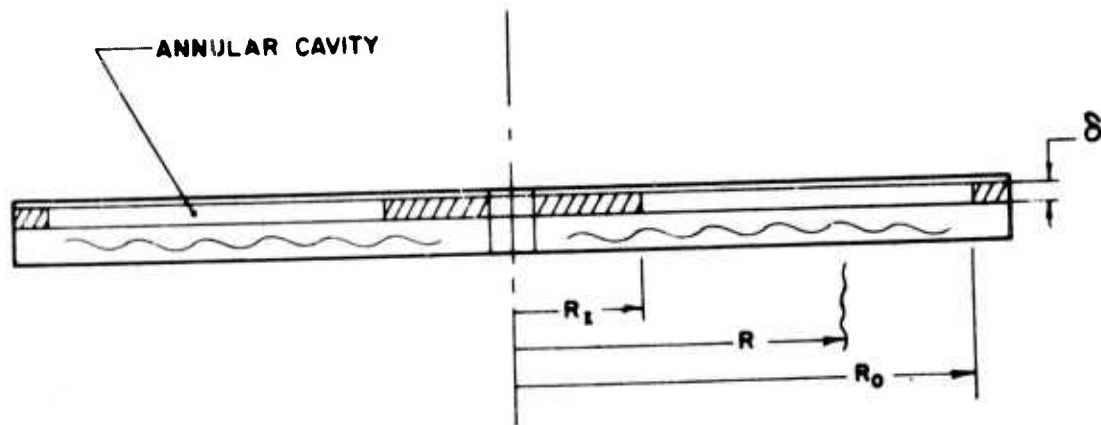


Figure 1: DRAW Air Sandwich Cavity

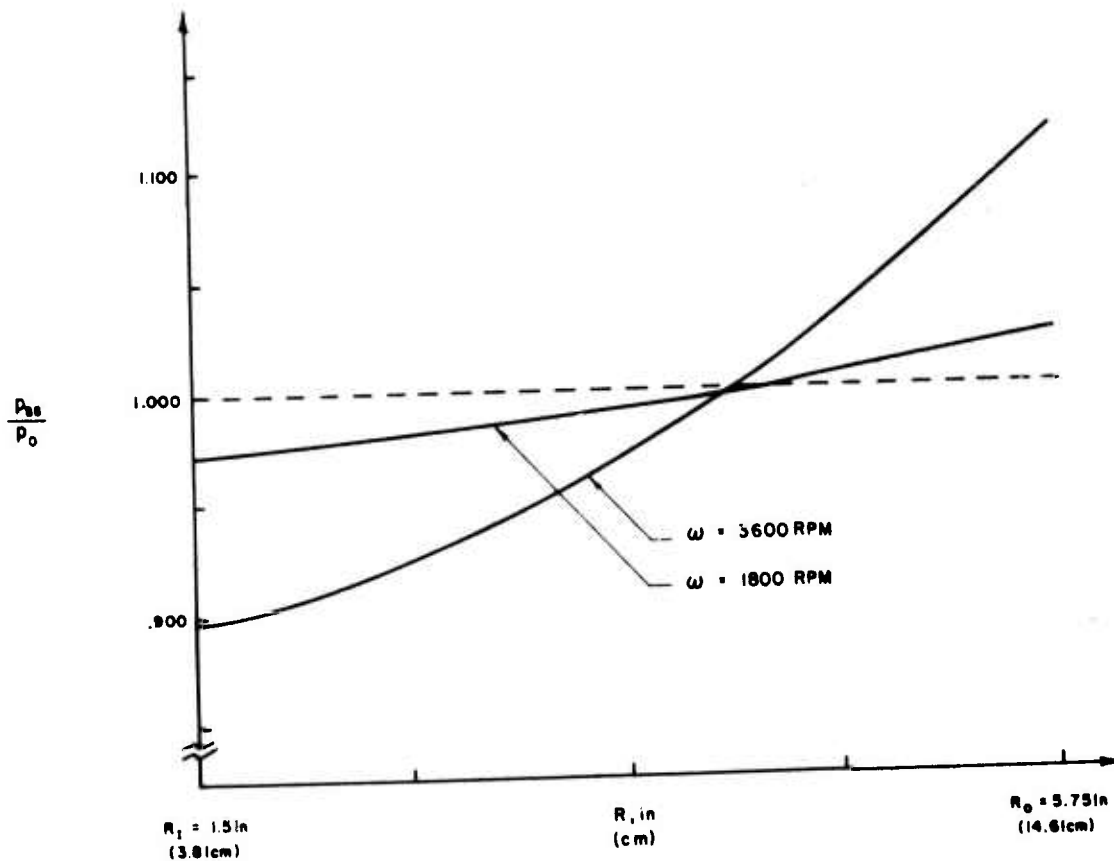


Figure 2: Pressure Distribution In a Rotating Hermetic Cavity

APPENDIX A

If expression (3) is set equal to a constant defined as C and differentiated with respect to r:

$$C_1 V \frac{\partial v}{\partial r} + \frac{M}{RTp} \frac{\partial p}{\partial r} = \frac{\partial C}{\partial r} \quad (\text{A-1})$$

The velocity V can now be replaced by  $\omega r$ , and the quantity  $C_1 \omega^2 r$  eliminated between equations (4) and (A-1):

$$\frac{\partial C}{\partial r} = \frac{1}{\rho} \frac{\partial p}{\partial r} + \frac{M}{RTp} \frac{\partial p}{\partial r} \quad (\text{A-2})$$

If the reciprocal density from equation (2) is substituted into equation (A-2):

$$\frac{\partial C}{\partial p} = \frac{1}{\rho} \frac{\partial p}{\partial r} \left( \frac{RT}{M} + \frac{M}{RT} \right) \quad (\text{A-3})$$

Finally, substitution of  $\partial C / \partial r$  from equation (A-3) into equation (A-1) yields:

$$\frac{dp}{p} = \frac{C_1 M}{RT} \omega^2 r dr \quad (\text{A-4})$$

APPENDIX B

From equation (2)

$$\rho_o = \frac{p_o M}{RT} \tag{B-1}$$

$$\rho_{ss} = \frac{p_{ss} M}{RT}$$

If  $\rho_o$  and  $\rho_{ss}$  are eliminated between equations (7) and (B-1):

$$p_o V_c = 2\pi\delta \int_{R_I}^{R_o} p_{ss} r dr \tag{B-2}$$

If  $p_{ss}$  from equation (6) is substituted into equation (B-2):

$$P_I = \frac{p_o V_c}{2\pi\delta \int_{R_I}^{R_o} r e^{\frac{C_1 M \omega^2}{2RT} (r - R_I^2)} dr} \tag{B-3}$$

The denominator of equation (B-3) can be evaluated as follows:

$$\int_{R_I}^{R_o} r e^{Ar^2 - AR_I^2} dr = e^{-AR_I^2} \int_{R_I}^{R_o} r e^{Ar^2} dr =$$

$$e^{-AR_I^2} \left. \begin{array}{l} Ar^2 \\ R_O \\ R_I \end{array} \right| = \frac{1}{2A} \left\{ e^{A(R_O^2 - R_I^2)} - 1 \right\}$$

where

$$A = \frac{C_1 M \omega^2}{2RT}$$

Therefore, if  $\pi (R_O^2 - R_I^2) \delta$  is substituted for the cavity volume, equation (B-3) becomes:

$$\frac{P_I}{P_O} = \frac{C_1 M \omega^2 (R_O^2 - R_I^2)}{2RT \left\{ e^{\frac{C_1 M \omega^2}{2RT} (R_O^2 - R_I^2)} - 1 \right\}} \quad (B-4)$$

The pressure  $p_I$  from equation (B-4) can now be substituted into equation (6). The result is equation (8).